Interaction of proliferating cell nuclear antigen with PMS2 is required for MutLα activation and function in mismatch repair

Jochen Genschel[a,b,1], Lyudmila Y. Kadyrova[c], Ravi R. Iyer[a,2], Basanta K. Dahal[c], Farid A. Kadyrov[c], and Paul Modrich[a,b,3]

[a]Department of Biochemistry, Duke University Medical Center, Durham, NC 27710; [b]Howard Hughes Medical Institute, Duke University Medical Center, Durham, NC 27710; and [c]Department of Biochemistry and Molecular Biology, Southern Illinois University School of Medicine, Carbondale, IL 62901

Contributed by Paul Modrich, March 22, 2017 (sent for review February 15, 2017; reviewed by Josef Jiricny, Guo-Min Li, and Michael O'Donnell)

Eukaryotic MutLα (mammalian MLH1–PMS2 heterodimer; MLH1–PMS1 in yeast) functions in early steps of mismatch repair as a latent endonuclease that requires a mismatch, MutSα/β, and DNA-loaded proliferating cell nuclear antigen (PCNA) for activation. We show here that human PCNA and MutLα interact specifically but weakly in solution to form a complex of approximately 1:1 stoichiometry that depends on PCNA interaction with the C-terminal endonuclease domain of the MutLα PMS2 subunit. Amino acid substitution mutations within a PMS2 C-terminal ^{721}QRLIAP motif attenuate or abolish human MutLα interaction with PCNA, as well as PCNA-dependent activation of MutLα endonuclease, PCNA- and DNA-dependent activation of MutLα ATPase, and MutLα function in in vitro mismatch repair. Amino acid substitution mutations within the corresponding yeast PMS1 motif (^{723}QKLIIP) reduce or abolish mismatch repair in vivo. Coupling of a weak allele within this motif (^{723}AKLIIP) with an *exo1*Δ null mutation, which individually confer only weak mutator phenotypes, inactivates mismatch repair in the yeast cell.

DNA repair | mismatch repair | MutLalpha | proliferating cell nuclear antigen | endonuclease

MutLα (mammalian MLH1–PMS2 heterodimer; MLH1–PMS1 in yeast) plays an essential role during early steps of eukaryotic mismatch repair (MMR) (1). Inactivation of the human protein is a cause of Lynch syndrome (2, 3), and has been implicated in the development of a subset of sporadic tumors (4). In physiological buffer (100 to 150 mM salt, 5 mM Mg^{2+}), MutLα functions as a latent, strand-directed endonuclease that depends on a mismatch, MutSα (MSH2–MSH6 heterodimer) or MutSβ (MSH2–MSH3 heterodimer), and the DNA-loaded form of the proliferating cell nuclear antigen (PCNA) sliding clamp for activation (5–8). Strand direction is conferred by the loading orientation of the PCNA clamp (8). Although not evident in physiological buffer, the intrinsic endonuclease activity of MutLα is demonstrable in the absence of other proteins provided the ionic strength is low and Mn^{2+} is substituted for Mg^{2+} (5, 6). Mn^{2+}-dependent nuclease activity does not respond to MutSα or a mismatch but is stimulated by loaded PCNA, suggesting that MutLα interaction with PCNA is required for the effect (6, 8). (Human MutLα, MLH1, PMS2, and PCNA, the primary subjects of this paper, are referred to as such in the text. For the purpose of distinction, yMutLα, yMLH1, yPMS1, and yPCNA are used for specific reference to the corresponding *Saccharomyces cerevisiae* proteins.)

The MutLα endonuclease center resides within the heterodimeric C-terminal domain (CTD) that is composed of the C-terminal domains of MLH1 and PMS2 (PMS1 in yeast) (9), and endonuclease function depends on the integrity of a $DQHA(X)_2E(X)_4E$ metal-binding active-site motif located within the PMS2/yPMS1 CTD (5, 6). The $DQHA(X)_2E(X)_4E$ endonuclease motif is also conserved in MutL proteins from bacteria that do not rely on d(GATC) methylation for strand direction of MMR, with *Bacillus subtilis* MutL the most extensively studied protein of this class. Like eukaryotic MutLα, *B. subtilis* MutL displays Mn^{2+}-dependent endonuclease activity that is stimulated by the bacterial β-sliding clamp (10). As in the case of eukaryotic MutLα, this effect presumably depends on physical interaction of the two proteins.

MutLα and PCNA have been shown to interact in both human and yeast systems (11–13). For *S. cerevisiae* proteins, PCNA interaction has been attributed to the yMLH1 subunit, and a conserved ^{572}QIGLTDF motif within the yMLH1 CTD has been suggested as a potential PCNA-interaction motif (11, 13). *B. subtilis* MutL and β-clamp have also been shown to form a transient complex in solution in a manner that depends on a QEMIVP motif within the CTD of the MutL homodimer, and moderately conserved variants of this element are found in the CTDs of PMS2 and yPMS1 (14). We show here that integrity of this element (^{721}QRLIAP) in the PMS2 CTD is required for normal PCNA–MutLα interaction, activation of MutLα endonuclease, and in vitro MMR. Integrity of the corresponding yPMS1 ^{723}QKLIIP is required for MMR in vivo. However, amino acid substitution within the human MLH1 CTD motif ^{562}QILIYDF, which corresponds to that invoked in yMLH1–yPCNA interaction, has little effect on PCNA–MutLα interaction or PCNA-dependent endonuclease activation, although MMR function of the mutant protein is impaired.

Significance

MutLα is required for initiation of eukaryotic mismatch repair. Inactivation of human MutLα is a cause of Lynch syndrome, a common hereditary cancer, and has also been implicated in the development of a subset of sporadic tumors. The proliferating cell nuclear antigen (PCNA) sliding clamp is required for activation and strand direction of the MutLα endonuclease. We show that physical interaction of the two proteins, which form a weak complex in solution, is required for MutLα activation, and have identified a hexapeptide motif within the MutLα PMS2 (PMS1 in yeast) subunit that is required for interaction with PCNA and for MutLα function in mismatch repair. These findings clarify the mechanism of MutLα activation and establish the importance of PCNA interaction in this process.

Author contributions: J.G., L.Y.K., R.R.I., F.A.K., and P.M. designed research; J.G., L.Y.K., R.R.I., B.K.D., and F.A.K. performed research; J.G., L.Y.K., R.R.I., B.K.D., F.A.K., and P.M. analyzed data; and J.G., F.A.K., and P.M. wrote the paper.

Reviewers: J.J., University of Zurich; G.-M.L., University of Southern California; and M.O., Rockefeller University.

The authors declare no conflict of interest.

Freely available online through the PNAS open access option.

[1]Present address: Precision BioSciences, Durham, NC 27701.

[2]Present address: Discovery and Product Development, Teva Branded Pharmaceutical Products R&D, West Chester, PA 19380.

[3]To whom correspondence should be addressed. Email: modrich@biochem.duke.edu.

This article contains supporting information online at www.pnas.org/lookup/suppl/doi:10.1073/pnas.1702561114/-/DCSupplemental.

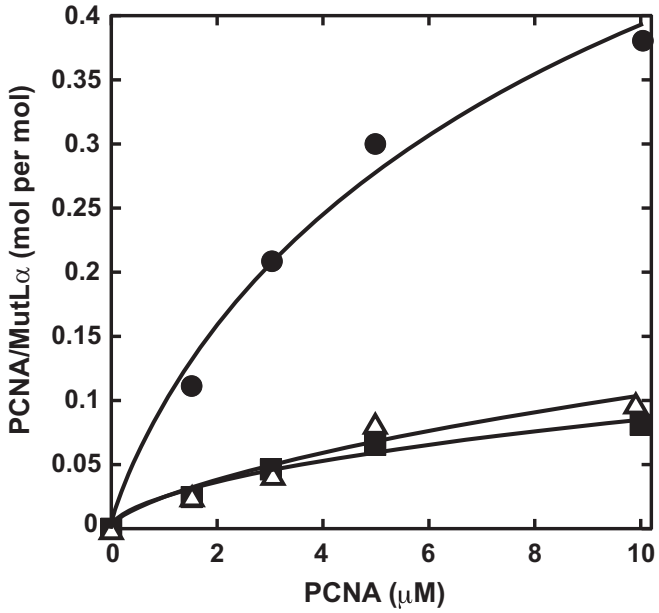

Fig. 1. PMS2 ^{721}QRLIA motif is required for MutLα interaction with PCNA in solution. Equilibrium gel filtration was performed (*Materials and Methods*) by injection of 10 μL 10 μM wild-type (circles), PMS2-Q721A (triangles), or PMS2-AAA (squares) MutLα onto a Superdex 200 column equilibrated with Hepes·KOH/KCl buffer and the indicated concentrations of PCNA. The curve for wild-type MutLα is a nonlinear regression fit to a multiligand binding isotherm (*Materials and Methods*). Best-fit parameters are K_d 7.7 μM and a stoichiometry of 0.8 PCNA trimer per MutLα. K_d and stoichiometry values for mutant proteins were not estimated due to the low level of binding.

Results

Human MutLα and PCNA Interact in Solution. We previously showed that human PCNA and MutLα interact as judged by far-Western blot (12), and confirm that conclusion here using equilibrium gel filtration (15). MutLα was injected onto Superdex 200 columns equilibrated with fixed concentrations of PCNA in physiological salt buffer containing Mg^{2+}. MutLα-bound sliding clamp was determined from the area of the trough at the PCNA retention volume that results from sequestration of the clamp by MutLα (Fig. S1*A*). Use of two independent preparations of MutLα and PCNA yielded apparent K_d values of 4.2 and 7.7 μM and stoichiometries of 1.1 and 0.8 PCNA trimers per MutLα heterodimer (Fig. 1 and Fig. S1*C*). Because these experiments were done under conditions of PCNA excess, they do not rule out potential multivalent interaction of the PCNA trimer with MutLα as might occur under conditions of MutLα excess, a possibility that was not addressed due to the prohibitive quantities of MutLα required for the analysis.

Physical interaction of PCNA and MutLα was also demonstrable by cross-linking with bis(sulfosuccinimidyl)suberate (BS^3; Fig. 2*A*, lanes 2 and 3). Analysis of the cross-linked species for peptide abundance by mass spectroscopy demonstrated that cross-linking by this agent is restricted to PCNA and the PMS2 subunit (Fig. 2*B*, open and filled blue bars). After normalization for molecular masses, cross-linking of PMS2 to PCNA under these conditions occurs at about 50% of the efficiency of PMS2 cross-linking to the MutLα MLH1 subunit.

Amino Acid Substitutions Within Putative PCNA-Binding Motifs: Implications for PCNA–MutLα Interaction. Lee and Alani (13) identified a highly conserved ^{572}QIGLTDF element within the CTD of *S. cerevisiae* MLH1 as a potential PCNA-interaction motif for yMutLα. Triple-Ala substitution within this motif (^{572}AIGATDA) was shown to confer a strong mutator phenotype and reduce yMutLα binding to yPCNA about twofold, as judged by surface plasmon resonance. Although this motif is similar to the canonical PCNA-interacting peptide motif (16), the recent structure of the yMutLα CTD (Fig. 3) has shown that this heptapeptide element is buried and unlikely to be involved in yPCNA interaction in the absence of a substantial conformational change (9). A second potential PCNA-interaction motif within the PMS2 CTD has been suggested by studies of the interaction of *B. subtilis* MutL with the β-clamp, an interaction that depends on a QEMIVP motif within the CTD of the MutL homodimer (14). Moderately conserved variants of this motif are found in the CTD of human PMS2 (^{721}QRLIAP) and yeast PMS1 (^{723}QKLIIP). Unlike the buried yMLH1 ^{572}QIGLTDF element, this yPMS1 motif is exposed as a surface loop (Fig. 3).

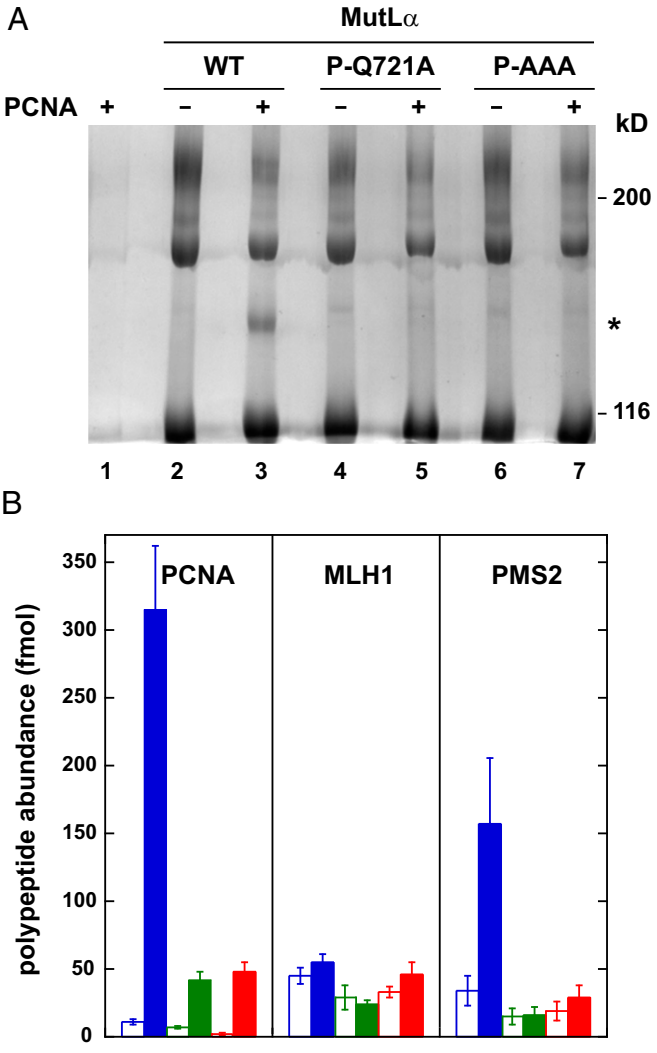

Fig. 2. BS^3 cross-linking of MutLα and PCNA. (*A*) Wild-type, PMS2-Q721A, or PMS2-AAA MutLα was cross-linked with BS^3 in the absence or presence of PCNA (*Materials and Methods*) and reaction products were resolved by SDS/PAGE and visualized with Coomassie brilliant blue. As judged by Western blot, the major cross-linked species with apparent mobility of 180 kDa corresponds to MLH1-PMS2. The cross-linked product of apparent mobility of 140 kDa (asterisk) is analyzed in *B*. (*B*) Mass spectroscopic quantification of PCNA, MLH1, and PMS2 tryptic peptides (*Materials and Methods*) derived from gel slices corresponding to the mobility of the 140-kDa cross-linked product produced with wild-type MutLα and PCNA, or the equivalent position in other lanes. Error bars are ±1 SD for wild-type MutLα (blue), PMS2-Q721A (green), and PMS2-AAA (red). Open and filled bars correspond to results obtained in the absence or presence of PCNA, respectively.

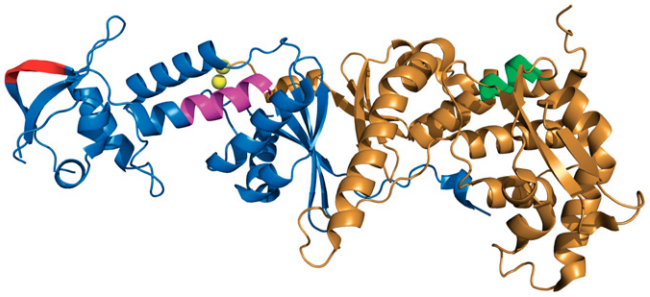

Fig. 3. Putative PCNA-binding motifs within the CTD of yeast MutLα. Structure of the C-terminal domain of *S. cerevisiae* MutLα (MLH1-PMS1) [Protein Data Bank ID code 4fmn (9)] as visualized with PyMOL (https://www.schrodinger.com). Structural elements shown are yPMS1 residues 651 to 873 (blue), yMLH1 residues 505 to 769 (brown), the yPMS1 endonuclease motif ^{701}DQHASDEKYNFE (magenta), two bound zinc ions (yellow), and putative PCNA-binding motifs within yPMS1 (^{723}QKLIIP; red) or MLH1 (^{572}QIGLTDF; green).

To address possible involvement of these elements in PCNA–MutLα interaction and endonuclease activation, we constructed human MutLα variants with amino acid substitution mutations within these motifs: MLH1 ^{562}QILIYDF → AILAYDA (MLH1-AAA), corresponding to the yMLH1 variant described above; PMS2 ^{721}QRLIAP → ^{721}ARLIAP (PMS2-Q721A); and ^{721}QRLIAP → ^{721}ARAAAP (PMS2-AAA). Human MLH1-AAA was coexpressed with wild-type PMS2, whereas PMS2-Q721A and PMS2-AAA were coexpressed with wild-type MLH1 (*Materials and Methods*). The three MutLα variants fractionate like wild-type MutLα and exhibit no obvious instability. The resulting MutLα heterodimers are referred to below as MLH1-AAA, PMS2-Q721A, and PMS2-AAA, respectively.

MutLα PMS2-Q721A and PMS2-AAA variants display greatly reduced affinity for PCNA as judged by equilibrium gel filtration (Fig. 1 and Fig. S1*B*), and no detectable cross-linking to the sliding clamp occurs in the presence of BS^3 (Fig. 2*A*, compare lanes 3, 5, and 7). By contrast, PCNA interaction with the MutLα MLH1-AAA variant does not differ significantly from that observed with wild-type MutLα, as judged by cross-linking assay (Fig. S2).

Implications for MMR and MutLα Activation. MLH1-AAA, PMS2-Q721A, and PMS2-AAA MutLα variants were compared with wild-type protein for their ability to restore MMR to extracts of MLH1$^{-/-}$ Exo1$^{-/-}$ mouse embryo fibroblast (MEF) cells in the presence of exogenous human exonuclease 1 (Exo1) (17). MLH1-AAA and PMS2-Q721A variants support significant residual activity as scored on either 3′ or 5′ G–T heteroduplex DNAs (20 to 30% or 10 to 20% residual activity, respectively), but triple-alanine substitution within the PMS2 ^{721}QRLIAP motif abolishes MutLα function in the extract repair assay (Table 1).

Table 1. Effects of amino acid substitutions within putative MutLα PCNA-interaction motifs on MutLα-dependent 3′- and 5′-directed MMR

	MutLα-dependent MMR, mol repaired/mol MutLα	
MutLα	3′ G–T	5′ G–T
WT	0.54 ± 0.04	0.39 ± 0.05
MLH1-AAA	0.11 ± 0.01	0.12 ± 0.01
PMS2-Q721A	0.06 ± 0.02	0.08 ± 0.01
PMS2-AAA	≤0.002	≤0.002

MMR was determined using 3′ or 5′ G–T heteroduplexes in repair-deficient whole-cell extract supplemented with variable MutLα concentrations (*Materials and Methods*). Errors are ±1 SD for triplicate determinations.

Table 2. Effects of amino acid substitutions within putative MutLα PCNA-interaction motifs on mismatch- and MutSα-dependent MutLα activation

MutLα	MutLα-dependent incision, mol incised/mol MutLα
WT	0.53 ± 0.08
MLH1-AAA	0.29 ± 0.01
PMS2-Q721A	0.18 ± 0.05
PMS2-AAA	≤0.01

Mismatch- and MutSα-dependent MutLα endonucleolytic incision was determined as a function of MutLα concentration using a 3′ G–T heteroduplex in physiological salt/Mg^{2+} buffer (*Materials and Methods*). Errors are ±1 SD. Background incision of homoduplex control DNA was 0.02 mol/mol for wild-type MutLα but undetectable in other cases.

The three variants were also compared with the wild-type protein for their ability to support strand-directed MutLα incision of 3′-nicked circular G–T heteroduplex DNA in Mg^{2+}/physiological salt buffer, where endonuclease activation depends on a mismatch, MutSα, PCNA, and RFC (5). As summarized in Table 2, MLH1-AAA and PMS2-Q721A variants retain significant residual endonuclease activity (60 and 30%, respectively) but activity of the PMS2-AAA MutLα variant is undetectable in this assay.

Because activation of the MutLα endonuclease and function of the protein in MMR depend on a network of protein interactions, we also tested the three variants for endonuclease function and activation in Mn^{2+}/low-salt buffer. MutLα endonuclease activity can be observed in the absence of other proteins under these conditions, and PCNA-dependent activation can be scored on homoduplex DNA (5, 6, 8). Incision of a 6.4-kb supercoiled homoduplex by PMS2-Q721A or PMS2-AAA MutLα variants in the absence of other proteins is indistinguishable from that mediated by the wild-type MutLα (Table 3), indicating that amino acid substitutions within the PMS2 ^{721}QRLIAP motif have negligible effect on inherent endonuclease active-site function. However, basal endonuclease activity of the MLH1-AAA variant is reduced 85% relative to wild-type MutLα. Given the physical distance between the MLH1 ^{562}QILIYDF motif and the endonuclease active site (Fig. 3), we attribute this activity reduction to conformational effects that span the two subunits.

As observed previously (5), incision of supercoiled DNA in Mn^{2+}/low-salt buffer by wild-type MutLα is dramatically enhanced by PCNA and RFC, increasing endonuclease specific activity more than 100-fold (Table 3). Despite the reduction in intrinsic active-site function, MLH1-AAA MutLα is also activated several hundred-fold by PCNA and RFC. By contrast, PCNA- and RFC-dependent activation of the PMS2-Q721A and PMS2-AAA MutLα variants is modest, with the extent of activation of the two proteins reduced 80 and 95%, respectively, compared with the wild-type heterodimer.

PCNA also activates the MutLα endonuclease on linear duplex DNA in Mn^{2+}/low-salt buffer but this activation is RFC-independent, presumably because the clamp can thread onto the end of the duplex (8). Wild type and the three MutLα variants were thus compared for hydrolytic activity on a 5′-fluorescently tagged 49-bp synthetic duplex. Incision of this short DNA by wild-type MutLα was demonstrable only in the presence of PCNA (Fig. S3), possibly due to the small target size. Furthermore, only one 5′-labeled product (~11 nt in length) was observed upon incision of either the top or bottom strand. Although the basis of this specificity was not pursued, it may indicate that binding of the hydrolytic complex to the small DNA is restricted to two productive conformations. As summarized in Table 4, PCNA-dependent incision of the small duplex by MLH1-AAA MutLα is nearly as robust as that observed with the wild-type heterodimer. However, activity of PMS2-Q721A MutLα and PMS2-AAA MutLα is dramatically compromised, with activity of the former variant reduced 90% relative to wild

Table 3. Amino acid substitutions within the PMS2 ^{721}QRLIAP motif impair PCNA- and RFC-dependent activation of the MutLα endonuclease on supercoiled DNA in the presence of Mn^{2+}

	MutLα-dependent incision, mol DNA incised/mol MutLα		Relative activation by PCNA/RFC
MutLα	−PCNA/RFC	+PCNA/RFC	
WT	0.13 ± 0.02	16 ± 2	123
MLH1-AAA	0.02 ± 0.01	5.5 ± 1	275
PMS2-Q721A	0.12 ± 0.02	3.1 ± 0.2	26
PMS2-AAA	0.12 ± 0.01	0.8 ± 0.3	7

Endonuclease activity on 6.4-kb supercoiled DNA was determined as a function of MutLα concentration under Mn^{2+}/low-salt conditions (*Materials and Methods*). PCNA and RFC preparations were free of detectable endonuclease activity. Values shown are ±1 SD for triplicate determinations.

type and activity of the latter being undetectable. Because PCNA and MutLα are the only proteins present in these experiments, the PMS2 ^{721}QRLIAP motif is clearly required for PCNA-dependent endonuclease activation but the MLH1 ^{562}QILIYDF element is not.

PCNA- and DNA-Dependent Modulation of MutLα ATPase. MutLα is a weak ATPase, and integrity of ATP hydrolytic centers within the N-terminal MLH1 and PMS2 domains is required for MMR (18). Although Räschle et al. (18) reported that MutLα ATP hydrolysis is unaffected by single-stranded DNA, we have found that ATP hydrolytic activity is stimulated by linear duplex DNA in low-salt buffer and that this effect is further potentiated by PCNA (Fig. 4). In the absence of DNA and PCNA, ATP hydrolysis by PMS2-Q721A and PMS2-AAA MutLα is indistinguishable from wild type (Fig. 4*A*, open symbols), and supplementation with PCNA is without effect (compare open symbols, Fig. 4 *A* and *B*). Supplementation with an excess of 49-bp duplex DNA activates hydrolysis by all three heterodimers to a comparable degree (Fig. 4*B*, closed symbols) and supplementation with both PCNA and 49-bp DNA further potentiates ATP hydrolysis, but in this case enhancement differs significantly for the three proteins, with wild type > PMS2-Q721A > PMS2-AAA (Fig. 4*A*). The apparent contribution of PCNA to DNA-dependent ATPase activation was estimated by subtraction of ATP hydrolytic activity observed in the presence of DNA alone from that observed in the presence of both cofactors (Fig. 4*C*). PCNA thus activates MutLα ATPase in a DNA-dependent manner, and the extent of activation correlates qualitatively with the effects of the PCNA substitution mutations on repair and endonuclease activation. Nevertheless, and despite the fact that the PMS2-AAA mutation virtually abolishes PCNA-dependent endonuclease activation, this variant apparently retains significant potential to respond to PCNA-dependent ATPase stimulation when DNA-bound (Fig. 4*C*, red squares). This suggests that the amino acid substitutions tested here do not completely abrogate clamp interaction with MutLα. The binding studies of Fig. 1 also suggest weak residual affinity of PCNA for the PMS2-Q721A and PMS2-AAA MutLα variants, although it is unclear whether this is due to residual affinity for the altered ^{721}QRLIAP motif or the presence of a weak secondary interaction site(s) within MutLα.

Genetic Consequences of Amino Acid Substitutions Within the Yeast PMS1 PCNA-Interaction Motif. Involvement of the MutLα PCNA-interaction element in MMR in vivo was addressed by constructing the corresponding substitutions (Q723A and Q723A, L725A, I726A) within the corresponding ^{723}QKLIIP motif of the *S. cerevisiae PMS1* chromosomal gene, which encodes the homolog of human PMS2. Mutabilities of these otherwise isogenic strains were then compared using *his7-2* and *lys2:InsE-A$_{14}$* frameshift reversion assays and the *CAN1* forward mutation assay. As shown in Table 5, the *pms1-Q723A* substitution results in significant but modest increases in mutation rates at all three reporter loci, consistent with a partial repair defect. However, the *pms1-AAA* triple-alanine substitution mutation results in dramatic mutation rate increases, similar to those observed in a *pms1*Δ strain.

The excision step of eukaryotic MMR is incompletely understood. Exonuclease 1 has been implicated in the pathway, but the modest mutation rate increase conferred by an Exo1 null mutation implies existence of at least one Exo1-independent mode of repair (1, 19). Biochemical and genetic experiments have suggested that MutLα endonuclease action plays an important role in Exo1-independent repair (17, 20), and additional support for this view is provided in Table 5. Although *exo1*Δ and *pms1-Q723A* mutations individually confer weak mutator phenotypes, they strongly synergize in a double mutant to increase the mutation rate to a degree comparable to that of a *pms1* null.

Discussion

Endonuclease action is a principal function of MutLα in MMR and depends on activation by a mismatch, MutSα or MutSβ, and DNA-loaded PCNA (5, 6, 8). Based on these previous studies, we inferred that physical interaction of MutLα with a loaded clamp is required for endonuclease activation. The experiments described here confirm this idea, demonstrating that a PMS2 ^{721}QRLIAP motif located within the MutLα C-terminal endonuclease domain plays an important role in physical interaction of the two proteins, and is required for both PCNA-dependent endonuclease activation and MutLα function in MMR.

This conclusion is strengthened by the fact that the consequences of amino acid substitutions within the ^{721}QRLIAP element are restricted to PCNA-dependent effects. Whereas substitutions within the hexapeptide motif reduce or abolish PCNA-dependent endonuclease activation as judged by several assays, they have no demonstrable effect on intrinsic endonuclease active-site function (Table 3). The ^{721}QRLIAP substitutions tested also have no effect on basal MutLα ATPase activity or the stimulation of basal ATPase by duplex DNA. They do, however, selectively attenuate PCNA-dependent ATPase activation that occurs in the presence of DNA (Fig. 4). These results are consistent with a mechanism whereby clamp interaction with the ^{721}QRLIAP element is conformationally transduced to DNA and ATP hydrolytic centers within C-terminal and N-terminal domains, respectively. They also suggest that the phenotypic consequences of the Ala substitutions that we have tested are largely restricted to selective interference with these processes. It is noteworthy that conformational interaction of N-terminal ATPase and C-terminal endonuclease domains is consistent with the finding that integrity of MutLα ATP hydrolytic centers is required for endonuclease activation (5) and with atomic force microscopy studies, which have demonstrated that ATP

Table 4. Effects of amino acid substitutions within putative MutLα PCNA-interaction motifs on the PCNA-dependent activation of the MutLα endonuclease with linear duplex DNA in the presence of Mn^{2+}

	PCNA activation of endonuclease activity, mol incision/mol PCNA	
MutLα	Top strand	Bottom strand
WT	0.17 ± 0.03	0.04 ± 0.02
MLH1-AAA	0.13 ± 0.04	0.03 ± 0.01
PMS2-Q721A	0.02 ± 0.004	≤0.002
PMS2-AAA	≤0.002	≤0.002

Endonuclease activity on 5′-fluorescently tagged 49-bp linear duplex was determined under Mn^{2+}/low-salt conditions as a function of PCNA concentration in the absence of RFC (*Materials and Methods*). Errors are ±1 SD for triplicate determinations. No detectable MutLα incision of this substrate was observed in the absence of PCNA (Fig. S3).

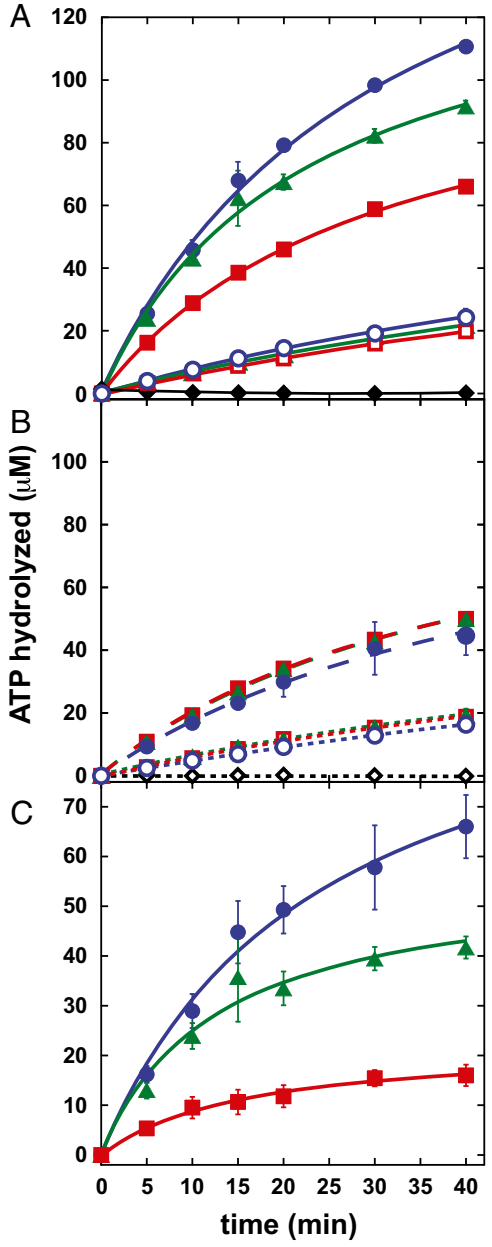

Fig. 4. PCNA- and DNA-dependent stimulation of MutLα ATPase is attenuated by amino acid substitutions within the PMS2 ^{721}QRLIAP motif. (*A*) ATP hydrolysis (*Materials and Methods*) by 0.68 μM wild-type MutLα (blue circles), MutLα PMS2-Q721A (green triangles), or MutLα PMS2-AAA (red squares) was determined in the absence (open symbols) or presence (closed symbols) of 1.4 μM PCNA and 2.1 μM 5′-phosphorylated 49-bp duplex DNA. ATP hydrolysis in the absence of MutLα but in the presence of 1.4 μM PCNA and 2.1 μM DNA was also determined (black diamonds). (*B*) As in *A*, but reactions contained either 0.68 μM MutLα and 2.1 μM DNA (closed symbols, broken lines) or 0.68 μM MutLα and 1.4 μM PCNA (open symbols, dotted lines). ATP hydrolysis by 1.4 μM PCNA alone is also shown (black diamonds). (*C*) Apparent PCNA-dependent stimulation of MutLα ATP hydrolysis was calculated as the difference between ATP hydrolysis observed in the presence of both PCNA and DNA (*A*, closed symbols) and that observed in the presence of DNA only (*B*, closed symbols). Symbols are as in *A*. Assays were done in triplicate, and error bars are ±1 SD. Error bars for *C* were computed as the square root of the quadratic sum of the individual SDs [$SD_C = (SD_A^2 + SD_B^2)^{1/2}$].

binding results in large conformational changes that may bring N- and C-terminal domains into proximity (21).

A ^{572}QIGLTDF motif within the C-terminal domain of yMLH1 has been postulated to play an important role in PCNA–yMutLα interaction (13), but we have found that triple-alanine substitution within the corresponding ^{562}QILIYDF human MLH1 heptapeptide has little effect on PCNA interaction with human MutLα (Fig. S2) and that PCNA activation of endonuclease function remains robust (Tables 3 and 4). The fact that the MLH1-AAA substitution reduces intrinsic function of the endonuclease active site by 85% (Table 3) indicates that this mutation has distal conformational consequences, and such effects may contribute to the reduced activity of this variant in MMR. It is nevertheless difficult to reconcile the magnitude of the repair defect that we observe in the human in vitro system (20 to 30% residual activity; Table 1) with that scored in vivo for the corresponding yeast mutation, which displays a mutability increase equivalent to that of an *mlh1*Δ (13). Functional ramifications of the MLH1-AAA mutation may therefore depend on sequence differences between the human and yeast proteins.

On the other hand, the genetic consequences of mutations within the yeast *PMS1* ^{723}QKLIIP element can be understood in terms of the in vitro functional effects of substitutions within the human PMS2 ^{721}QRLIAP motif. The modest mutability conferred by the *S. cerevisiae pms1-Q723A* mutation (Table 5) is consistent with the fact that PMS2-Q721A MutLα retains 10 to 20% MMR function (Table 1) and responds to PCNA activation with 10 to 30% of the efficiency of the wild-type protein (Tables 2–4). The high mutability conferred by the yeast *pms1-AAA* mutation is also in agreement with the molecular properties of PMS2-AAA MutLα, which is virtually defective in both PCNA activation and MMR (Tables 1–4).

MutLα endonuclease action has been previously implicated in MMR that occurs in the absence of Exo1. MMR in extracts of Exo1-deficient mouse cells requires MutLα endonuclease function and apparently occurs by a mechanism that does not involve an obligatory gapped intermediate, an effect attributed to synthesis-driven strand displacement by DNA polymerase δ (17). Yeast genetic studies have also shown that when present on a low-copy-number plasmid, yPMS1 endonuclease active-site mutations have weak dominant-negative effects on repair in a wild-type background but stronger negative effects in an *exo1* null context (20). Our finding that *pms1-Q723A* and *exo1*Δ mutations strongly synergize in a hypermutation assay (Table 5) is also consistent with MutLα function in Exo1-independent repair, and in particular is indicative of the importance of PCNA-dependent endonuclease activation in this process.

In vitro study of eukaryotic mismatch repair has relied on use of a strand-specific nick or gap to direct heteroduplex correction, with DNA termini at the discontinuities presumably serving as molecular signals for the reaction (1). Such DNAs support two types of strand-directed reactions in vitro: 5′-to-3′ hydrolytic mismatch removal by MutSα- or MutSβ-activated Exo1 (22, 23), and strand-directed incision by activated MutLα endonuclease (5). Genetic studies indicate that 5′-to-3′ mismatch removal by activated Exo1 may function preferentially on the lagging strand at the fork, suggesting that Okazaki fragment 5′ termini may serve as loading sites for the exonuclease (24).

It is also clear that a primary activity of MutLα in mismatch repair is its function as a strand-directed endonuclease. Amino acid substitutions within the MutLα endonuclease active site abolish mismatch repair both in vitro and in vivo, although they have no demonstrable effect on MutLα ATP hydrolytic activity or assembly of the MutLα–MutSα–heteroduplex ternary complex (5, 6). Although the identity of the biological strand signals that direct MutLα endonuclease action has not been established, the fact that strand direction is provided by loaded PCNA (8) suggests several possibilities. PCNA loaded at 3′ termini on leading and lagging strands at the fork would presumably suffice in this regard provided that MutLα could access such clamps, either directly or after remodeling of the replication complex. DNA strand breaks produced by RNase H2 incision at sites of misincorporated ribonucleotides have also been invoked as strand signals for mismatch repair, particularly on the leading strand (25, 26). Although the contribution of such events to strand direction appears to be limited, given the modest mutability of yeast strains deficient in RNase H2 (25–27), DNA

Table 5. Effects of *pms1-Q723A* and *pms1-AAA*[a] mutations on genome stability in haploid yeast *S. cerevisiae*

	Mutation rate					
	his7-2		*lys2:InsE-A$_{14}$*		*Can^r*	
Relevant genotype	Absolute rate, $\times10^{-8}$	Relative rate	Absolute rate, $\times10^{-8}$	Relative rate	Absolute rate, $\times10^{-8}$	Relative rate
Wild type	0.6* (0.6 to 1.0)	1	22 (15 to 28)	1	19* (16 to 24)	1
pms1Δ	120 (110 to 160)	200	160,000 (130,000 to 190,000)	7,300	580 (480 to 690)	31
pms1-Q723A	7.0 (5.6 to 9.5)	12	6,200 (5,700 to 8,200)	280	42 (39 to 55)	2
pms1-AAA[†]	150 (130 to 190)	250	120,000 (84,000 to 130,000)	5,500	500 (400 to 760)	26
pms1-Q723A exo1Δ	270 (130 to 340)	450	120,000 (86,000 to 150,000)	5,500	820 (560 to 1200)	43
exo1Δ	2.9 (1.9 to 5.7)	5	540 (430 to 740)	25	120 (90 to 220)	6

The strains are E134 (wild type) (30) and its mutant derivatives; 95% confidence intervals are in parentheses. Rate shown as mutations per cell division.
*Data are from a previous report (32).
[†]*pms1-AAA* corresponds to Q723A, L725A, I726A alanine substitutions.

strand breaks produced in this manner could function as secondary sites for loading of PCNA or MutSα-activated Exo1.

Materials and Methods

Proteins, Extracts, and DNAs. Proteins were isolated and MEF whole-cell extracts were prepared as described (12, 17, 22). MLH1 and PMS2 mutants were constructed by PCR mutagenesis of the pFastbacI expression vectors for wild-type proteins (28) and confirmed by sequencing of entire reading frames. G–T heteroduplexes containing a strand break located 128 bp either 3′ or 5′ of the mismatch were prepared from phages f1MR70 and f1MR71 (29). Details are provided in *SI Materials and Methods*.

Equilibrium Gel Filtration and Protein Cross-Linking. Physical interaction of PCNA with MutLα was scored by equilibrium gel filtration (15) on a Superdex 200 column equilibrated with variable PCNA concentrations and by protein–protein cross-linking with bis(sulfosuccinimidyl)suberate (Thermo Scientific). Cross-linked products were analyzed by Western blot using commercial antibodies against MLH1, PMS2, and PCNA, or by quadrupole mass spectroscopy after excision from polyacrylamide gels and trypsin digestion. Details are provided in *SI Materials and Methods*.

MMR, Endonuclease, and ATPase Assays. In vitro MMR was determined using 6.4-kb circular G–T heteroduplexes with a strand break located 128 nt 3′ or 5′ of the mismatch and whole-cell extracts derived from Exo1$^{-/-}$ MLH1$^{-/-}$ MEF cells that were supplemented with Exo1 and MutLα as indicated (17, 29). Strand-directed activation of the MutLα endonuclease was determined using a 6.4-kb 3′ G–T heteroduplex in physiological salt (5 mM Mg^{2+}, 100 mM KCl) in the presence of MutSα, RFC, PCNA, RPA, and MutLα as indicated (5). MutLα activation under reduced specificity conditions (1 mM Mn^{2+}, 25 mM KCl) was scored as a function of MutLα concentration on 6.4-kb supercoiled circular homoduplex DNA in the absence or presence of PCNA and RFC, or on 49-bp linear duplex DNA in the absence or presence of PCNA (5, 8). ATP hydrolysis by MutLα (18) was determined in the absence of cofactors, presence of 49-bp duplex DNA, or presence of 49-bp duplex DNA and PCNA. Details are provided in *SI Materials and Methods*.

Yeast Strains and Genetic Methods. *S. cerevisiae* strains analyzed in this study were derivatives of the haploid wild-type strain E134 (*MATα ade5-1 lys2::InsE-A$_{14}$ trp1-289 his7-2 leu2-3,112 ura3-52*) (30). *exo1Δ* and *pms1Δ* null mutants were constructed by transformation with replacement cassettes, whereas *pms1-Q723A* and *pms1-Q723A,L725A,I726A* alleles were prepared by the *delitto perfetto* method (31). Spontaneous mutation rates were determined as described (32). Details are provided in *SI Materials and Methods*.

ACKNOWLEDGMENTS. This work was supported in part by NIH Grants GM045190 (to P.M.) and GM095758 (to F.A.K.). P.M. is an Investigator of the Howard Hughes Medical Institute.

1. Jiricny J (2013) Postreplicative mismatch repair. *Cold Spring Harb Perspect Biol* 5:a012633.
2. Peltomäki P (2003) Role of DNA mismatch repair defects in the pathogenesis of human cancer. *J Clin Oncol* 21:1174–1179.
3. Rowley PT (2005) Inherited susceptibility to colorectal cancer. *Annu Rev Med* 56:539–554.
4. Jacinto FV, Esteller M (2007) Mutator pathways unleashed by epigenetic silencing in human cancer. *Mutagenesis* 22:247–253.
5. Kadyrov FA, Dzantiev L, Constantin N, Modrich P (2006) Endonucleolytic function of MutLalpha in human mismatch repair. *Cell* 126:297–308.
6. Kadyrov FA, et al. (2007) *Saccharomyces cerevisiae* MutLalpha is a mismatch repair endonuclease. *J Biol Chem* 282:37181–37190.
7. Iyer RR, et al. (2010) MutLalpha and proliferating cell nuclear antigen share binding sites on MutSbeta. *J Biol Chem* 285:11730–11739.
8. Pluciennik A, et al. (2010) PCNA function in the activation and strand direction of MutLα endonuclease in mismatch repair. *Proc Natl Acad Sci USA* 107:16066–16071.
9. Gueneau E, et al. (2013) Structure of the MutLα C-terminal domain reveals how Mlh1 contributes to Pms1 endonuclease site. *Nat Struct Mol Biol* 20:461–468.
10. Pillon MC, et al. (2015) The sliding clamp tethers the endonuclease domain of MutL to DNA. *Nucleic Acids Res* 43:10746–10759.
11. Umar A, et al. (1996) Requirement for PCNA in DNA mismatch repair at a step preceding DNA resynthesis. *Cell* 87:65–73.
12. Dzantiev L, et al. (2004) A defined human system that supports bidirectional mismatch-provoked excision. *Mol Cell* 15:31–41.
13. Lee SD, Alani E (2006) Analysis of interactions between mismatch repair initiation factors and the replication processivity factor PCNA. *J Mol Biol* 355:175–184.
14. Pillon MC, Miller JH, Guarné A (2011) The endonuclease domain of MutL interacts with the β sliding clamp. *DNA Repair (Amst)* 10:87–93.
15. Ackers GK (1973) Studies of protein ligand binding by gel permeation techniques. *Methods Enzymol* 27:441–455.
16. Warbrick E (1998) PCNA binding through a conserved motif. *BioEssays* 20:195–199.
17. Kadyrov FA, et al. (2009) A possible mechanism for exonuclease 1-independent eukaryotic mismatch repair. *Proc Natl Acad Sci USA* 106:8495–8500.
18. Räschle M, Dufner P, Marra G, Jiricny J (2002) Mutations within the hMLH1 and hPMS2 subunits of the human MutLalpha mismatch repair factor affect its ATPase activity, but not its ability to interact with hMutSalpha. *J Biol Chem* 277:21810–21820.
19. Goellner EM, Putnam CD, Kolodner RD (2015) Exonuclease 1-dependent and independent mismatch repair. *DNA Repair (Amst)* 32:24–32.
20. Smith CE, et al. (2013) Dominant mutations in *S. cerevisiae* PMS1 identify the Mlh1-Pms1 endonuclease active site and an exonuclease 1-independent mismatch repair pathway. *PLoS Genet* 9:e1003869.
21. Sacho EJ, Kadyrov FA, Modrich P, Kunkel TA, Erie DA (2008) Direct visualization of asymmetric adenine-nucleotide-induced conformational changes in MutL alpha. *Mol Cell* 29:112–121.
22. Genschel J, Modrich P (2003) Mechanism of 5′-directed excision in human mismatch repair. *Mol Cell* 12:1077–1086.
23. Zhang Y, et al. (2005) Reconstitution of 5′-directed human mismatch repair in a purified system. *Cell* 122:693–705.
24. Liberti SE, Larrea AA, Kunkel TA (2013) Exonuclease 1 preferentially repairs mismatches generated by DNA polymerase α. *DNA Repair (Amst)* 12:92–96.
25. Ghodgaonkar MM, et al. (2013) Ribonucleotides misincorporated into DNA act as strand-discrimination signals in eukaryotic mismatch repair. *Mol Cell* 50:323–332.
26. Lujan SA, Williams JS, Clausen AR, Clark AB, Kunkel TA (2013) Ribonucleotides are signals for mismatch repair of leading-strand replication errors. *Mol Cell* 50:437–443.
27. Allen-Soltero S, Martinez SL, Putnam CD, Kolodner RD (2014) A *Saccharomyces cerevisiae* RNase H2 interaction network functions to suppress genome instability. *Mol Cell Biol* 34:1521–1534.
28. Blackwell LJ, Wang S, Modrich P (2001) DNA chain length dependence of formation and dynamics of hMutSalpha.hMutLalpha.heteroduplex complexes. *J Biol Chem* 276:33233–33240.
29. Genschel J, Modrich P (2009) Functions of MutLalpha, replication protein A (RPA), and HMGB1 in 5′-directed mismatch repair. *J Biol Chem* 284:21536–21544.
30. Tran HT, Keen JD, Kricker M, Resnick MA, Gordenin DA (1997) Hypermutability of homonucleotide runs in mismatch repair and DNA polymerase proofreading yeast mutants. *Mol Cell Biol* 17:2859–2865.
31. Storici F, Resnick MA (2006) The delitto perfetto approach to in vivo site-directed mutagenesis and chromosome rearrangements with synthetic oligonucleotides in yeast. *Methods Enzymol* 409:329–345.
32. Kadyrova LY, et al. (2013) A reversible histone H3 acetylation cooperates with mismatch repair and replicative polymerases in maintaining genome stability. *PLoS Genet* 9:e1003899.